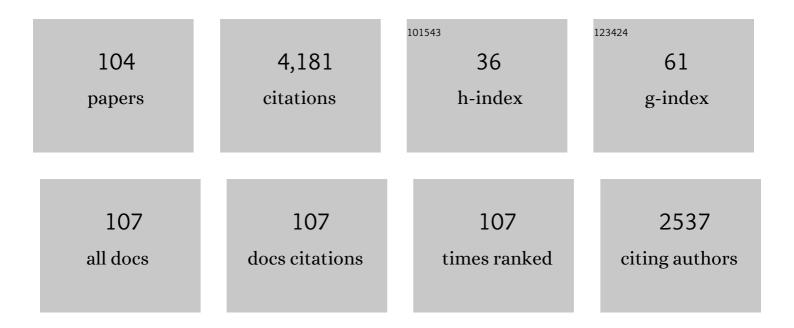
Bharat Gwalani

List of Publications by Year in descending order

Source: https://exaly.com/author-pdf/3842584/publications.pdf Version: 2024-02-01



#	Article	IF	CITATIONS
1	Optimizing the coupled effects of Hall-Petch and precipitation strengthening in a Al 0.3 CoCrFeNi high entropy alloy. Materials and Design, 2017, 121, 254-260.	7.0	287
2	A combinatorial assessment of AlxCrCuFeNi2 (0Â<ÂxÂ<Â1.5) complex concentrated alloys: Microstructure, microhardness, and magnetic properties. Acta Materialia, 2016, 116, 63-76.	7.9	219
3	Modifying transformation pathways in high entropy alloys or complex concentrated alloys via thermo-mechanical processing. Acta Materialia, 2018, 153, 169-185.	7.9	169
4	Stability of ordered L12 and B2 precipitates in face centered cubic based high entropy alloys - Al0.3CoFeCrNi and Al0.3CuFeCrNi2. Scripta Materialia, 2016, 123, 130-134.	5.2	165
5	Enhancing strength and strain hardenability via deformation twinning in fcc-based high entropy alloys reinforced with intermetallic compounds. Acta Materialia, 2019, 165, 420-430.	7.9	155
6	Microstructural Design for Improving Ductility of An Initially Brittle Refractory High Entropy Alloy. Scientific Reports, 2018, 8, 8816.	3.3	138
7	Tensile yield strength of a single bulk Al0.3CoCrFeNi high entropy alloy can be tuned from 160â€⁻MPa to 1800â€⁻MPa. Scripta Materialia, 2019, 162, 18-23.	5.2	138
8	Cu assisted stabilization and nucleation of L12 precipitates in Al0.3CuFeCrNi2 fcc-based high entropy alloy. Acta Materialia, 2017, 129, 170-182.	7.9	130
9	Phase inversion in a two-phase, BCC+B2, refractory high entropy alloy. Acta Materialia, 2020, 185, 89-97.	7.9	128
10	Hierarchical features infused heterogeneous grain structure for extraordinary strength-ductility synergy. Materials Research Letters, 2018, 6, 676-682.	8.7	103
11	Fatigue behavior of ultrafine grained triplex Al0.3CoCrFeNi high entropy alloy. Scripta Materialia, 2019, 158, 116-120.	5.2	101
12	Contrasting mechanical behavior in precipitation hardenable AlXCoCrFeNi high entropy alloy microstructures: Single phase FCC vs. dual phase FCC-BCC. Materials Science & Engineering A: Structural Materials: Properties, Microstructure and Processing, 2019, 739, 158-166.	5.6	97
13	A Combinatorial Approach for Assessing the Magnetic Properties of High Entropy Alloys: Role of Cr in AlCo _{<i>x</i>} Cr _{1–<i>x</i>} FeNi. Advanced Engineering Materials, 2017, 19, 1700048.	3.5	95
14	Formation of a Huesler-like L21 phase in a CoCrCuFeNiAlTi high-entropy alloy. Scripta Materialia, 2015, 100, 36-39.	5.2	93
15	Change in the primary solidification phase from fcc to bcc -based B2 in high entropy or complex concentrated alloys. Scripta Materialia, 2017, 127, 186-190.	5.2	85
16	Reciprocating sliding wear behavior of high entropy alloys in dry and marine environments. Materials Chemistry and Physics, 2018, 210, 162-169.	4.0	82
17	Phase stability as a function of temperature in a refractory high-entropy alloy. Journal of Materials Research, 2018, 33, 3235-3246.	2.6	80
18	High performance rechargeable Li-S batteries using binder-free large sulfur-loaded three-dimensional carbon nanotubes. Carbon, 2017, 118, 120-126.	10.3	70

#	Article	IF	CITATIONS
19	Microstructures and mechanical properties of mechanically alloyed and spark plasma sintered Al0.3CoCrFeMnNi high entropy alloy. Materials Chemistry and Physics, 2018, 210, 62-70.	4.0	63
20	Phase stability and microstructure evolution in a ductile refractory high entropy alloy Al10Nb15Ta5Ti30Zr40. Materialia, 2020, 9, 100569.	2.7	61
21	Influence of ordered L12 precipitation on strain-rate dependent mechanical behavior in a eutectic high entropy alloy. Scientific Reports, 2019, 9, 6371.	3.3	59
22	High density of strong yet deformable intermetallic nanorods leads to an excellent room temperature strength-ductility combination in a high entropy alloy. Acta Materialia, 2021, 219, 117234.	7.9	59
23	Engineering multi-scale B2 precipitation in a heterogeneous FCC based microstructure to enhance the mechanical properties of a Al0.5Co1.5CrFeNi1.5 high entropy alloy. Journal of Alloys and Compounds, 2020, 830, 154707.	5.5	57
24	High-entropy alloy strengthened by in situ formation of entropy-stabilized nano-dispersoids. Scientific Reports, 2018, 8, 14085.	3.3	55
25	Laser additive manufacturing of compositionally graded AlCrFeMoVx (x = 0 to 1) high-entropy alloy system. Optics and Laser Technology, 2019, 113, 330-337.	4.6	55
26	Microstructure and wear resistance of an intermetallic-based Al0.25Ti0.75CoCrFeNi high entropy alloy. Materials Chemistry and Physics, 2018, 210, 197-206.	4.0	53
27	Strengthening of Al0.3CoCrFeMnNi-based ODS high entropy alloys with incremental changes in the concentration of Y2O3. Scripta Materialia, 2019, 162, 477-481.	5.2	52
28	Microstructure and mechanical behavior of an additive manufactured (AM) WE43-Mg alloy. Additive Manufacturing, 2019, 26, 53-64.	3.0	50
29	Tuning the phase stability and magnetic properties of laser additively processed Fe-30at%Ni soft magnetic alloys. Materials Letters, 2017, 199, 88-92.	2.6	49
30	Grain size dependence of strain rate sensitivity in a single phase FCC high entropy alloy Al0.3CoCrFeNi. Materials Science & Engineering A: Structural Materials: Properties, Microstructure and Processing, 2018, 736, 344-348.	5.6	49
31	Recovery of cold-worked Al0.3CoCrFeNi complex concentrated alloy through twinning assisted B2 precipitation. Acta Materialia, 2021, 202, 448-462.	7.9	47
32	Microstructures with extraordinary dynamic work hardening and strain rate sensitivity in Al0.3CoCrFeNi high entropy alloy. Materials Science & Engineering A: Structural Materials: Properties, Microstructure and Processing, 2018, 734, 42-50.	5.6	46
33	Experimental investigation of the ordering pathway in a Ni-33Âat.%Cr alloy. Acta Materialia, 2016, 115, 372-384.	7.9	42
34	Crystallographically degenerate B2 precipitation in a plastically deformed <i>fcc</i> -based complex concentrated alloy. Materials Research Letters, 2018, 6, 171-177.	8.7	40
35	The effect of cold rolling on grain boundary structure and stress corrosion cracking susceptibility of twins in alloy 690 in simulated PWR primary water environment. Corrosion Science, 2018, 130, 126-137.	6.6	40
36	Influence of non-magnetic Cu on enhancing the low temperature magnetic properties and Curie temperature of FeCoNiCrCu(x) high entropy alloys. Scripta Materialia, 2020, 182, 99-103.	5.2	40

#	Article	IF	CITATIONS
37	Development of in situ composites via reactive friction stir processing of Ti–B4C system. Composites Part B: Engineering, 2019, 172, 54-60.	12.0	38
38	On the role of Ag in enhanced age hardening kinetics of Mg–Gd–Ag–Zr alloys. Philosophical Magazine Letters, 2016, 96, 212-219.	1.2	36
39	Deformation Induced Hierarchical Twinning Coupled with Omega Transformation in a Metastable β-Ti Alloy. Scientific Reports, 2019, 9, 1334.	3.3	36
40	Influence of Cr Substitution and Temperature on Hierarchical Phase Decomposition in the AlCoFeNi High Entropy Alloy. Scientific Reports, 2018, 8, 15578.	3.3	34
41	Microstructural dependence of strain rate sensitivity in thermomechanically processed Al0.1CoCrFeNi high entropy alloy. Materials Science & Engineering A: Structural Materials: Properties, Microstructure and Processing, 2018, 727, 148-159.	5.6	33
42	Hierarchical multi-scale microstructural evolution in an as-cast Al2CuCrFeNi2 complex concentrated alloy. Intermetallics, 2016, 71, 31-42.	3.9	31
43	Surface degradation mechanisms in precipitation-hardened high-entropy alloys. Npj Materials Degradation, 2018, 2, .	5.8	31
44	Role of copper on L12 precipitation strengthened fcc based high entropy alloy. Materialia, 2019, 6, 100282.	2.7	31
45	Discontinuous precipitation leading to nano-rod intermetallic precipitates in an Al0.2Ti0.3Co1.5CrFeNi1.5 high entropy alloy results in an excellent strength-ductility combination. Materials Science & amp; Engineering A: Structural Materials: Properties, Microstructure and Processing, 2021, 805, 140551.	5.6	31
46	Extreme shear-deformation-induced modification of defect structures and hierarchical microstructure in an Al–Si alloy. Communications Materials, 2020, 1, .	6.9	29
47	Tuning the degree of chemical ordering in the solid solution of a complex concentrated alloy and its impact on mechanical properties. Acta Materialia, 2021, 212, 116938.	7.9	29
48	Effect of nano-sized precipitates on the fatigue property of a lamellar structured high entropy alloy. Materials Science & Engineering A: Structural Materials: Properties, Microstructure and Processing, 2019, 760, 225-230.	5.6	28
49	Hierarchical Eutectoid Nano-lamellar Decomposition in an Al0.3CoFeNi Complex Concentrated Alloy. Scientific Reports, 2020, 10, 4836.	3.3	27
50	Effect of reactive alloy elements on friction stir welded butt joints of metallurgically immiscible magnesium alloys and steel. Journal of Manufacturing Processes, 2019, 39, 138-145.	5.9	26
51	Interplay between single phase solid solution strengthening and multi-phase strengthening in the same high entropy alloy. Materials Science & Engineering A: Structural Materials: Properties, Microstructure and Processing, 2020, 771, 138620.	5.6	26
52	Composition-dependent apparent activation-energy and sluggish grain-growth in high entropy alloys. Materials Research Letters, 2019, 7, 267-274.	8.7	25
53	Influence of fine-scale B2 precipitation on dynamic compression and wear properties in hypo-eutectic Al0.5CoCrFeNi high-entropy alloy. Journal of Alloys and Compounds, 2021, 853, 157126.	5.5	21
54	Ordering-mediated local nano-clustering results in unusually large Hall-Petch strengthening coefficients in high entropy alloys. Materials Research Letters, 2021, 9, 213-222.	8.7	21

#	Article	IF	CITATIONS
55	Deformation induced intermediate metastable lattice structures facilitate ordered B2 nucleation in a fcc-based high entropy alloy. Materials Research Letters, 2019, 7, 40-46.	8.7	20
56	The evolution of microstructure and microhardness in a biomedical Ti–35Nb–7Zr–5Ta alloy. Journal of Materials Science, 2017, 52, 3062-3073.	3.7	18
57	Compositionally graded high entropy alloy with a strong front and ductile back. Materials Today Communications, 2019. 20, 100602, constrained and oxidation behaviour of two high- <mml:math< td=""><td>1.9</td><td>18</td></mml:math<>	1.9	18
58	xmlns:mml="http://www.w3.org/1998/Math/MathML" altimg="si1.gif" display="inline" overflow="scroll"> < mml:msup> < mml:mrow> < mml:mi mathvariant="normal"> î³ < /mml:mi> < /mml:mrow> < mml:mrow> < mml:mo>′ < /mml:mo> < /mml:mrow> < /mml:m W-free < mml:math xmlns:mml="http://www.w3.org/1998/Math/MathML" altimg="si12.gif"	ւsu p ∞/mr	nl:math>
59	display="inline" overflow="scroll"> <mml:mi mathyariant="normal">î³<mml:msup><mml:mrow Highly tunable magnetic and mechanical properties in an Al0.3CoFeNi complex concentrated alloy. Materialia, 2020, 12, 100755.</mml:mrow </mml:msup></mml:mi 	2.7	17
60	Nanomechanical scratching induced local shear deformation and microstructural evolution in single crystal copper. Applied Surface Science, 2021, 562, 150132.	6.1	17
61	Hierarchical phase evolution in a lamellar Al0.7CoCrFeNi high entropy alloy involving competing metastable and stable phases. Scripta Materialia, 2021, 204, 114137.	5.2	17
62	Pine Wood Extracted Activated Carbon through Selfâ€Activation Process for Highâ€Performance Lithiumâ€Ion Battery. ChemistrySelect, 2016, 1, 4000-4007.	1.5	16
63	Dynamic Shear Deformation of a Precipitation Hardened Al0.7CoCrFeNi Eutectic High-Entropy Alloy Using Hat-Shaped Specimen Geometry. Entropy, 2020, 22, 431.	2.2	16
64	Rapid assessment of structural and compositional changes during early stages of zirconium alloy oxidation. Npj Materials Degradation, 2020, 4, .	5.8	14
65	Lattice misorientation evolution and grain refinement in Al-Si alloys under high-strain shear deformation. Materialia, 2021, 18, 101146.	2.7	14
66	Excellent ballistic impact resistance of Al0.3CoCrFeNi multi-principal element alloy with unique bimodal microstructure. Scientific Reports, 2021, 11, 22715.	3.3	14
67	Immiscible nanostructured copper-aluminum-niobium alloy with excellent precipitation strengthening upon friction stir processing and aging. Scripta Materialia, 2019, 164, 42-47.	5.2	13
68	Molecular-scale investigation of the oxidation behavior of chromia-forming alloys in high-temperature CO2. Npj Materials Degradation, 2021, 5, .	5.8	13
69	Facile Photochemical Syntheses of Conjoined Nanotwin Gold-Silver Particles within a Biologically-Benign Chitosan Polymer. Nanomaterials, 2019, 9, 596.	4.1	12
70	Engineering transformation pathways in an Al _{0.3} CoFeNi complex concentrated alloy leads to excellent strength–ductility combination. Materials Research Letters, 2020, 8, 399-407.	8.7	12
71	Shear strain gradient in Cu/Nb nanolaminates: Strain accommodation and chemical mixing. Acta Materialia, 2022, 234, 117986.	7.9	12
72	A novel nano-particle strengthened titanium alloy with exceptional specific strength. Scientific Reports, 2019, 9, 11726.	3.3	11

#	Article	IF	CITATIONS
73	High oxidation resistance of AlCoCrFeNi high entropy alloy through severe shear deformation processing. Journal of Alloys and Compounds, 2022, 917, 165385.	5.5	11
74	Microstructure and mechanical properties of friction stir processed cast Eglin steel (ES-1). Materials Science & Engineering A: Structural Materials: Properties, Microstructure and Processing, 2018, 709, 105-114.	5.6	10
75	Multimodal analysis of spatially heterogeneous microstructural refinement and softening mechanisms in three-pass friction stir processed Al-4Si alloy. Journal of Alloys and Compounds, 2021, 887, 161351.	5.5	9
76	Thermal stability and mechanical properties of cold-sprayed Nickel-Yttria coating. Scripta Materialia, 2022, 207, 114281.	5.2	9
77	Co-introduction of precipitate hardening and TRIP in a TWIP high-entropy alloy using friction stir alloying. Scientific Reports, 2021, 11, 1579.	3.3	8
78	Highly complex magnetic behavior resulting from hierarchical phase separation in AlCo(Cr)FeNi high-entropy alloys. IScience, 2022, 25, 104047.	4.1	8
79	Microstructural Assessment of a Multiple-Intermetallic-Strengthened Aluminum Alloy Produced from Gas-Atomized Powder by Hot Extrusion and Friction Extrusion. Materials, 2020, 13, 5333.	2.9	7
80	Deformation behavior of metallic glass composites and plasticity accommodation at microstructural length-scales. Materials Today Communications, 2020, 24, 101237.	1.9	6
81	Mechanistic insights into selective oxidation and corrosion of multi-principal element alloys from high resolution and in situ microscopy. Materialia, 2021, 18, 101148.	2.7	6
82	In-situ TEM observation of shear induced microstructure evolution in Cu-Nb alloy. Scripta Materialia, 2021, 205, 114214.	5.2	6
83	Phase transformations, microstructural refinement and defect evolution mechanisms in Al-Si alloys under non-hydrostatic diamond anvil cell compression. Materialia, 2021, 15, 101049.	2.7	5
84	Insights into Defect-Mediated Nucleation of Equilibrium B2 Phase in Face-Centered Cubic High-Entropy Alloys. Jom, 2021, 73, 2320-2331.	1.9	5
85	Atomistic understanding of extreme strain shear deformation of Copper-Graphene composites. Carbon, 2022, 198, 63-69.	10.3	5
86	Additively Manufactured Functionally Graded FeNi based High Entropy Magnetic Alloys. , 2018, , .		4
87	High Strain Rate Response of Al0.7CoCrFeNi High Entropy Alloy: Dynamic Strength Over 2ÂGPa from Thermomechanical Processing and Hierarchical Microstructure. Journal of Dynamic Behavior of Materials, 2019, 5, 1-7.	1.7	4
88	Formation and dissociation of shear-induced high-energy dislocations: insight from molecular dynamics simulations. Modelling and Simulation in Materials Science and Engineering, 2022, 30, 025012.	2.0	4
89	Detailed Investigation of Core–Shell Precipitates in a Cu-Containing High Entropy Alloy. Jom, 2018, 70, 1771-1775.	1.9	3
90	Decoupling of strain and temperature effects on microstructural evolution during high shear strain deformation. Materialia, 2022, 22, 101402.	2.7	3

6

#	Article	IF	CITATIONS
91	Metallurgical joining of immiscible system: Pure Mg and pure Fe. Materials Characterization, 2022, 187, 111821.	4.4	3
92	Extended Shear Deformation of the Immiscible Cu–Nb Alloy Resulting in Nanostructuring and Oxygen Ingress with Enhancement in Mechanical Properties. ACS Omega, 2022, 7, 13721-13736.	3.5	3
93	Designing and characterizing a complex concentrated gamma/gamma prime â€~superalloy'. Microscopy and Microanalysis, 2016, 22, 672-673.	0.4	2
94	Simulation of solute clusters in metallic systems. Modelling and Simulation in Materials Science and Engineering, 2019, 27, 085014.	2.0	1
95	Understanding the microstructural stability in a γ′-strengthened Ni-Fe-Cr-Al-Ti alloy. Journal of Alloys and Compounds, 2021, 886, 161207.	5.5	1
96	Grain Boundary Precipitation in Ni Based Superalloy 690 Investigated via Site-specific Atom Probe Microscopy. Microscopy and Microanalysis, 2016, 22, 1500-1501.	0.4	0
97	Investigation of Clusters and Their Effect on Grain Growth in Single Phase AlxCoCrFeNi High Entropy Alloys. Microscopy and Microanalysis, 2018, 24, 2214-2215.	0.4	0
98	Direct Observation of Zirconium Alloy Oxidation at the Nanoscale. Microscopy and Microanalysis, 2019, 25, 318-319.	0.4	0
99	Multimodal Atomic Scale Characterization of Structural and Compositional Changes During Shear Deformation of Materials. Microscopy and Microanalysis, 2019, 25, 2510-2511.	0.4	0
100	Influence of Composition and Structure on Measured H Concentration in beta-Ti Alloys via Atom Probe Tomography. Microscopy and Microanalysis, 2019, 25, 2542-2543.	0.4	0
101	Shear-Deformation-Induced Modification of Defect Structures and Hierarchical Microstructures in Miscible and Immiscible Alloys. Microscopy and Microanalysis, 2021, 27, 3106-3108.	0.4	0
102	In-situ TEM observation of bending induced sub-grain boundary formation in copper single crystal. Microscopy and Microanalysis, 2021, 27, 3414-3415.	0.4	0
103	Phase Transformations, Microstructural Refinement and Defect Evolution Mechanisms in Al-Si Alloys Under Non-Hydrostatic Diamond Anvil Cell Compression. SSRN Electronic Journal, 0, , .	0.4	0
104	An Approach for the Microstructure-Sensitive Simulation of Shear-Induced Deformation and Recrystallization in Al–Si Alloys. Metallurgical and Materials Transactions A: Physical Metallurgy and Materials Science, 2022, 53, 1450.	2.2	0